Phase change material-enhanced shoe sole for foot thermal regulation to prevent hyperthermia

H. Nemati[1], Roozbeh Naemi[2]

[1]Department of Mechanics, Marvdasht Branch, Islamic Azad University, Marvdasht, Iran.

Corresponding Author: H.Nemati@miau.ac.ir

[2]Centre for Biomechanics and Rehabilitation Technologies, Staffordshire University, Leek Road, Stoke on Trent ST4 2DF, UK

Abstract

Along with the aesthetics and comfort of the shoes, the thermal characteristics of the shoes are one of the most important factors that should be considered in their design. In weight-bearing activities of daily living, the foot plantar temperature can increase considerably which can be uncomfortable and lead to injuries. Most literature has focused on the mechanical behavior of the shoe sole to accommodate cushioning. In this study, a shoe sole design that can accommodate appropriate thermal properties to prevent excessive foot temperature rise during activities of daily living was investigated.

As it is challenging to find a material that has both suitable thermal and mechanical properties, in this study, a Phase Change Material (PCM) -enhanced shoe sole was innovated and proposed. In this design, a structured porous layer is embedded inside the shoe sole, in which the pore space is filled with PCM. Different low-temperature PCMs were proposed and simulated. Among them, paraffin wax (RT35) and PEG 900 showed outstanding performance. It was shown that using these PCM-enhanced shoe soles can keep foot soles cool, after 30 minutes of slow walking. These sole designs were also effective in keeping the foot sole cool during intensive activities like jogging or running.

Keywords: Footwear, Thermal comfort, Plantar soft tissue temperature, PCM, Hyperthermia, Diabetic Foot

1. Introduction

The thermal characteristics of footwear are contributing factors to the shoe performance that shall be taken into account in conjunction with its aesthetics and comfort[1, 2]. In the human body, only a few percent of energy (around 20~50% [3]) is converted to mechanical work and the rest is dissipated in the form of heat. Meanwhile, the foot sole as the body radiator [4] plays an important role in thermoregulation and cooling[5-7]. Consequently, footwear shall not prevent the cooling role of a foot sole, especially in intense physical activities like running in which, the foot sole temperature during warm summer days can reach 50°C or even higher [8]. Foot thermal regulation is more important in conditions such as diabetes as excess foot temperature is associated with an increase in the risk of diabetic foot ulcers [9-11].

Although a temperature above 35°C is uncomfortable [12, 13], few analytical or numerical works can be found with a focus on the solutions for cooling the foot. Based on the experimental works of Shimazaki et al. [14-17], Nemati et al. [18]proposed an analytical method to predict the foot sole temperature during running/jogging at different speeds, considering both the mechanical and thermal properties of the shoe soles. In that study, a good agreement between the predicted and the measured temperatures at the ball of the foot was reported [18]. In the same study, in contrast to the temperature at the ball of the foot, the measured arch temperature did not rise at the same rate and consequently, it deviated after a while from the predicted temperature[18]. The arch temperature can be 2 to 3°C less than the ball temperature and this difference in temperature rise can be due to the effect of sweating in the arch area as highlighted in Nemati et al. [18]. In another study, Nemati and Naemi developed an analytical model where another source term was considered in the energy equation to simulate the sweating effect[19]. The results of that study indicated that whereas the ball temperature is not affected by sweating, it is an effective mechanism in cooling the arch area and needs to be considered as a source of thermal regulation at the foot [19].In addition to the variations in heat exchanges of different parts of the foot due to the sweating effect, the foot temperature is also affected by the amount of heat transfer through the sole of the shoe [18].

Comparing the results of simulations for two shoe soles from EVA08 and EVA12 (with shore hardnesses of A45 and A35 respectively), showed that EVA12 is softer and maybe more comfortable[14-17]. However, the foot sole maximum temperature rise in a shoe made from EVA12 is around 3°C higher than EVA08which is due to the higher heat capacity of EVA08 compared to EVA12[18]. This example shows that suitable mechanical and thermal properties for a shoe sole may not be gathered in a single material and to accommodate thermal requirements there is a need for specified materials.

Phase Change Material (PCM) is a substance that stores and releases a great amount of thermal energy mostly in the form of latent heat within a narrow temperature change [20-22]. So, a PCM-enhanced shoe sole can potentially be used to accommodate foot sole thermal regulation. During an intensive activity, PCM can store dissipated heat from the shoe sole within a limited temperature rise and release it later. Generally, concerning the melting temperature, PCMs can be categorized into two main groups. In the first group, there is a single point for melting and solidification. So, until there is a solid core in the medium, the surrounding temperature remains constant at that melting temperature. In contrast, for the PCMs in the second group, there is a narrow range for melting temperature. Consequently, the surrounding medium temperature is not constant and varies within the melting temperature range.

Besides selecting a proper PCM among different available materials, it is important to use PCM in a way that does not affect the weight and mechanical properties of the shoe sole. This study aims to investigate the effect of using a PCM-enhanced shoe sole, in regulating foot temperature.

The first objective of this study was to propose a design to embed PCM inside the sole of the shoe without changing the mechanical properties of the shoe sole that can potentially affect the walking dynamics. This is important because the mechanical properties of a PCM change during the melting from solid to liquid. So, appropriate design considerations need to be taken into account to accommodate such changes and to ensure the integrity of the shoe sole. The second objective was to propose different PCMs and simulate the effect of those on the foot temperature during different levels of activity using the analytical models. Melting temperature, as well as single or narrow range melting point of different PCMs, can affect the thermal regulation performance of the shoe and the temperature of the foot during weight-bearing activities of daily living which have not been previously investigated. The third objective of this study was to estimate the maximum value of foot sole temperature rise in the presence of each PCM and comparing that, with the shoe sole complex made of conventional materials and finally, the last objective was to determine the adequate amount of PCM that is necessary to keep feet cool during daily walking or intense physical activities such as running or jogging.

2. Model development

In this study, we proposed to use PCM inside a layer of a structured porous medium (Fig. 1). Structured porous medium shows a superior thermal property[23]. In this design, a structured coarse porous media is embedded between two solid layers, while the pores are filled with a PCM (Fig. 1). Coarse pores shall be set up to stand the mechanical loads during the activity (Fig. 1). In a structured porous media, a basic shape is repeated to construct the porous media[23]. The two solid layers act as load distributers to uniformly distribute the load over the foot sole surface (Fig. 1).

Figure 1 shows the schematic of a foot in footwear. As shown in this figure, the dissipated heat from the foot sole (q''_{met}) is transferred via conduction through the shoe sole and then to the ambient via convection.

The shoe sole is divided into three layers, i.e. two solid layers and a structured porous layer in the middle. The porous layer is composed of studs distributed uniformly over the shoe sole surface. In this study, the total shoe sole thickness is 20 mm adopted from experiments of Shimazaki et al. [14-17]. The thicknesses of the lower and upper solid layers are selected as 12 mm and 3 mm, respectively. So, 5 mm remains for porous layer thickness. The bottom layer was selected much thicker to reduce the risk of perforation and spilling of PCM.

Studs in the porous layer are 2×2 mm with a height of 5 mm and pitch of 6 mm. With this arrangement, the porosity of the layer is 88.9%. The free spaces between studs are filled with PCM. By choosing a proper PCM, the temperature will not rise beyond the PCM melting point. Because at the melting point, PCM starts melting and heat is stored in the form of latent heat.

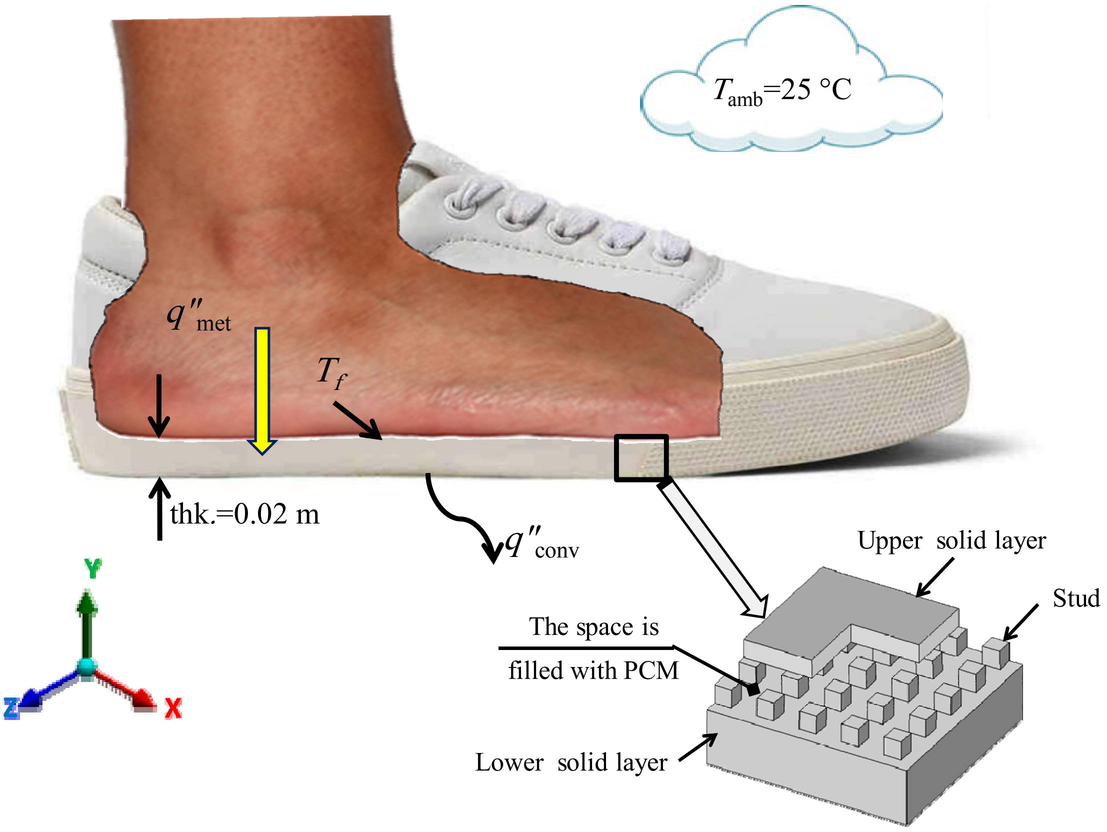

Fig. 1: Schematic of a foot, in a shoe and a zoom-in view of PCM-enhanced shoe sole.

Governing equations, i.e. continuity, momentum, and energy equations are:

- Continuity equation:

$$\nabla.\vec{v} = 0 \tag{1}$$

- Momentum-conservation equation:

$$\frac{\partial(\vec{v})}{\partial\tau} + \vec{v}.\nabla(\vec{v}) = 1/\rho\big(-\nabla P + \mu\nabla^2(\vec{v}) + \vec{g}\beta(T - T_l)\big) + S \tag{2}$$

where T_l is PCM melting temperature and $\vec{g} = [0, -9.81, 0]$ is the gravity vector. To model the buoyancy in the above equations, the Boussinesq approximation [24] was utilized.

- Energy-conservation equation for PCM:

$$\frac{\partial(H)}{\partial\tau} + \nabla.(\vec{v}H) = \nabla.(\frac{k}{\rho}\nabla T) \tag{3}$$

Generally, there are two models to simulate melting: moving boundary and fixed grid [25-28]. In this study, the “enthalpy-porosity method” was used to simulate the PCM melting with a fixed grid [29]. In this method, the following source term is added to the momentum equation to inhibit the motion of the solid PCM:

$$S = \frac{C(1-\gamma)^2}{(\gamma^3 + \epsilon)}\vec{v} \tag{4}$$

where $\epsilon = 0.001$ is a small number used to avoid an indeterminate division. $C = 10^5$ is a large constant and shows the amplitude of the damping. The liquid fraction, γ, is defined as:

$$\gamma = \begin{cases} 0 & \text{for} \quad T < T_s \\ \dfrac{T - T_s}{T_l - T_s} & \text{for} \quad T_s \le T \le T_l \\ 1 & \text{for} \quad T > T_l \end{cases} \tag{5}$$

where T_s and T_l are the solidification and melting temperatures, respectively.

The enthalpy of the PCM, H, is composed of both the sensible enthalpy, h, and the latent heat:

$$H = H_{ref} + \int_{T_{\text{ref}}}^{T} c_p dT \tag{6}$$

and

$$\Delta H = \gamma L \tag{7}$$

where H_{ref} is the enthalpy of PCM at the reference temperature ($T_{\mathrm{ref}} = 298.15$ K).

- Energy-conservation equation for solid:

$$\frac{1}{\alpha_s}\frac{\partial(T)}{\partial t} = \nabla^2 T \tag{8}$$

To solve the governing equations, the ANSYS-Fluent solver module of ANSYS 19.1 was used. The PISO (Pressure-Implicit with Splitting of Operators) scheme was selected for the pressure-velocity coupling [30] and the second-order upwind method was utilized to discretize energy and momentum equations. The first-order implicit method was used for time discretization. Residuals were set to 10^{-4} for continuity and momentum, 10^{-6} for the energy equation.

The experiment of Chen et al. [31] was used to validate the above procedure. The comparison of simulation results with experimental data is shown in Fig. 2 and very good agreement is observed. As a result, the same procedure is used to simulate PCM melting inside the shoe sole.

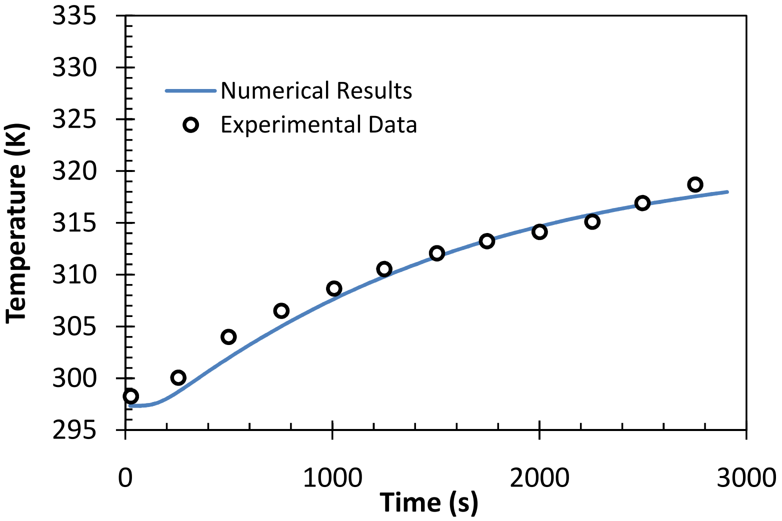

Fig. 2: Comparison of the average temperature with the experimental results of [31].

3. Data Analysis

Based on the experimental works of Shimazaki et al.[15], several candidates wore the shoes without socks and stood for a long time (around 10 minutes). In that study, the experiments were performed in a climate chamber with air at a constant temperature of 25°C, 50% *RH*, and no wind and solar load[15]. The shoe was a running shoe with a woven upper. The shoe sole was from EVA80 with a length of 26cm. Thermo-physical properties of EVA80 are presented in Table 1.

Table 1: EVA08thermo-physical properties [17]

c_{ps} [kJ/kgK]	k_s [W/mK]	ρ_s [kg/m^3]
2.585	0.11	240

At this stage, the measured average temperature of the foot sole was 34°C. Knowing the temperature of both sides of the shoe sole, the heat flux at the steady-state condition before the beginning of running is 49.5 W[18]. With the start of running for 30 min., the heat dissipation from the foot sole increases by a factor F[18]:

$$F(V) = 1.3\frac{0.009V^2 + 0.002V + 0.082}{0.009V_{\text{ref}}^2 + 0.002V_{\text{ref}} + 0.082} \tag{9}$$

V_{ref} is 0.833 m/s (3 km/hr).

During running, heat is transferred through convection from the outsole of the shoe (q''_{conv}). Assuming the outsole as a flat surface, the average convection coefficient (h) is [32]:

$$h = 0.037\frac{k_a}{l}Re^{4/5}Pr^{1/3}$$

$$Re = \frac{\rho_a . V . l}{\mu} \tag{10}$$

$$Pr = \frac{\mu_a . c_{pa}}{k_a}$$

where $l = 0.26$ m is the shoe outsole length and V is running velocity. In the above equation:

$$Re = \frac{\rho_a . V . l}{\mu} \tag{11}$$

$$Pr = \frac{\mu_a . c_{pa}}{k_a} \tag{12}$$

Air thermo-physical properties are presented in Table 2.

Table 2: Air thermo-physical properties at 25 [32]

Temperature (°C)	c_{p_a} [kJ/kg K]	k_a [W/mK]	ρ_a [kg/m^3]	μ_a [Pa.s]
25	1.007	0.0261	1.171	1.84E-5

For the shoe with a standard shoe sole, equations were solved numerically. Ball temperature rise, as well as those from experimental measurements, are presented in Fig. 3.

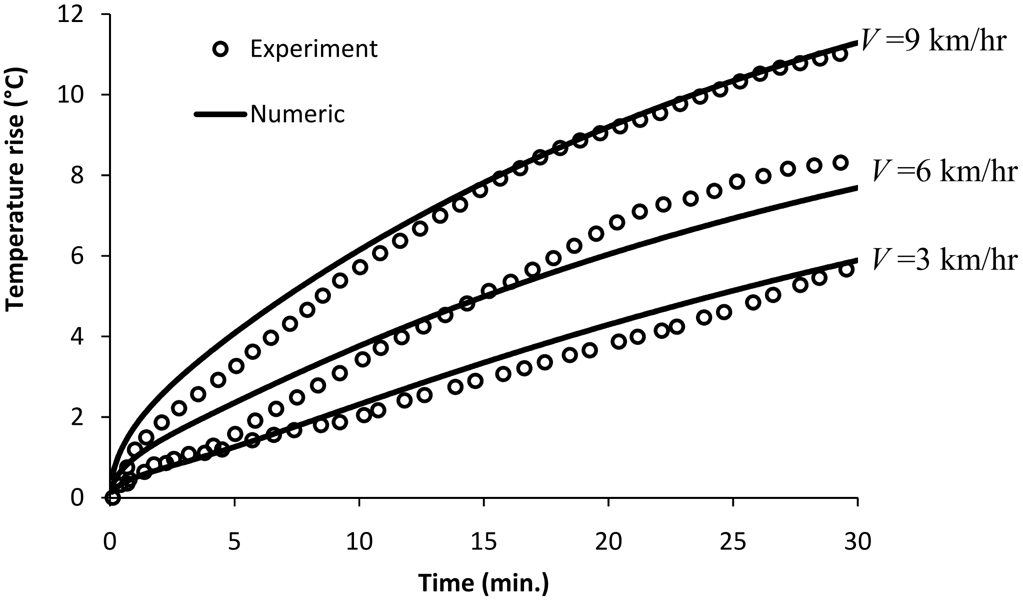

Fig. 3: Comparison of temperature rise at the ball of the foot (numerical simulation and experimental measurements).

Numerical and experimental results are in good agreement with each other. Based on this figure, at the highest gait speed i.e. 9 km/hr, the ball temperature has risen about 11°C which is not comfortable.

Based on the numerical results, at the initial state, the temperature at the interface of the upper solid layer and porous layer is something about 33°C. So, to avoid the PCM melting and to reserve its thermal storage capacity, the melting temperature must be more than 33°C. Furthermore, since a foot temperature above 35°C is uncomfortable [12, 13], the melting temperature shall be less than 38~40 °C. It must also be effective for low-speed walking like 3 km/hr. On the other hand, PCM shall not be harmful to human skin.

Considering all the above conditions, a few materials can be found suitable. Table 3 presents the list of candidates for them, the melting temperature is between 33–38 °C. Most of these PCMs are fatty acids[33, 34].The first few ones have narrow-range melting temperatures and the last three ones have single-point melting temperatures.

Table 3: The thermos-physical properties of PCMs

Property	$T_s - T_l$[°C]	Latent heat (L) [kJ/kg]	Ref.
RT35 (Paraffin Wax)	**32 – 38**	**160**	**[35]**
Lauric-palmitic acids (66%:34%)	33.4 – 36.5	169.2	[36]
Lauric-palmitic acids (67%:33%)	34.1 – 36.1	168.4	[36]
Lauric-palmitic acids (68%:32%)	34.7 – 35.5	167.7	[36]
Lauric-palmitic acids (70%:30%)	36.0 – 37.3	165.6	[36]
Polyethylene glycol 900 (PEG 900)	**34**	**150.5**	**[37]**
Lauric-palmitic acids (69%:31%)	35.2	166.3	[36]
Lauric-Stearic Acids (75.5%:24.5%)	**37**	**182.7**	**[38]**

For this study, three organic PCM materials from what was presented in Table 3 -shown in bold- were selected. The first one is a paraffin wax (RT35) with a melting point between 32–38°C (from the group of narrow-range melting temperatures). The second one (L-S acids) is a eutectic mixture of lauric and stearic acids (fatty acids). The binary mixture of the lauric and stearic acids with a weight percent of 75.5%:24.5% forms a eutectic, which melts in a single point temperature of 37°C with no subcooling during solidification. This melting point is close to the upper limit of paraffin wax melting temperature. Finally, the third one is PEG900 with a single-point melting temperature close to the lower limit of paraffin wax melting temperature. The properties of selected PCMs are presented in Table 4.

Table 4: The thermo-physical properties of PCMs

Property	RT35 (Paraffin Wax) [35]	Lauric-Stearic Acids (75.5%:24.5%) [38]	PEG900 [37]
$T_s - T_l$ [°C]	32 – 38	37	34
Density (ρ) [kg/m3]	860 – 770	990 – 894.2	1100 – 1120
Thermal conductivity (k) [W/mK]	0.2	0.18	0.188
Specific heat (c_p) [kJ/kg K]	2	1.92–2.1	2.26
Latent heat (L) [kJ/kg]	160	182.7	150.5
Dynamic viscosity μ [Pa.s]	0.0031	0.0078	0.0016
Volumetric thermal expansion coefficient β [1/K]	0.00125	---	0.00076

The thermal properties of all PCMs are close to each other. However, paraffin melts in a temperature range whereas the mixture of the fatty acid (L-S) and PEG 900 melt at a single-point temperature.

Fig. 4 shows the foot sole temperature rise relative to the initial temperature for the case of the standard shoe sole, i.e., 34 °C. Based on these figures, at the beginning of the running, the ball temperature is slightly colder than the standard shoe sole (less than 1°C).Because the total heat capacity of solid PCMs (ρc_p) is considerably more than EVA08. So, the small layer of PCM slightly improves the thermal performance of the shoe sole. In low-speed walking (i.e. 3 km/hr), the temperature in the paraffin-enhanced sole is under control as the onset of melting is at 32 °C, melting commences from the early stages of walking and consequently, after 30 minutes, the temperature rise is less than 2 °C. So, using RT35 provides an appropriate thermal condition during walking. In contrast, the L-S acids-enhanced sole only relies on sensible heat storage and not latent heat storage, since the temperature is lower than the melting point. As a result, the foot sole temperature is only around 3 °C colder than the standard shoe. PEG900 performance is in between these two above cases. Before the first 18 minutes, the thermal behavior of PEG900 is more similar to L-S acids. However, at the start of the melting period, the temperature remains constant and after 30 minutes of jogging, the foot sole temperature is more than 4 °C colder than when using a standard shoe sole. In conclusion, L-S acids cannot be commended for common walking shoes.

Conditions for high-velocity jogging (6 km/hr) are more or less similar to 3 km/hr. But, in this case, PEG 900 melting starts at the earlier stages, at about the thirteenth minute.

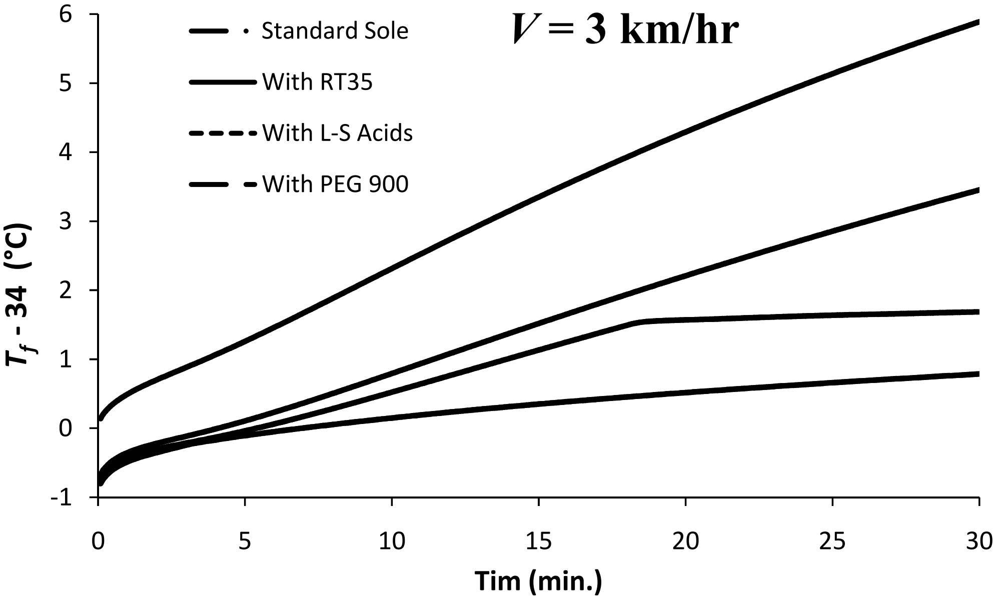

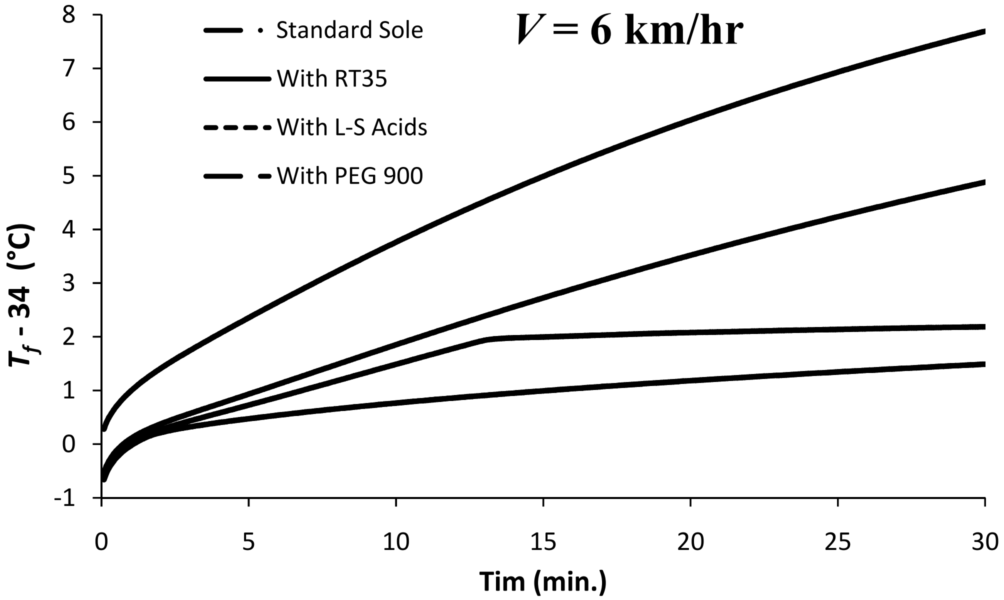

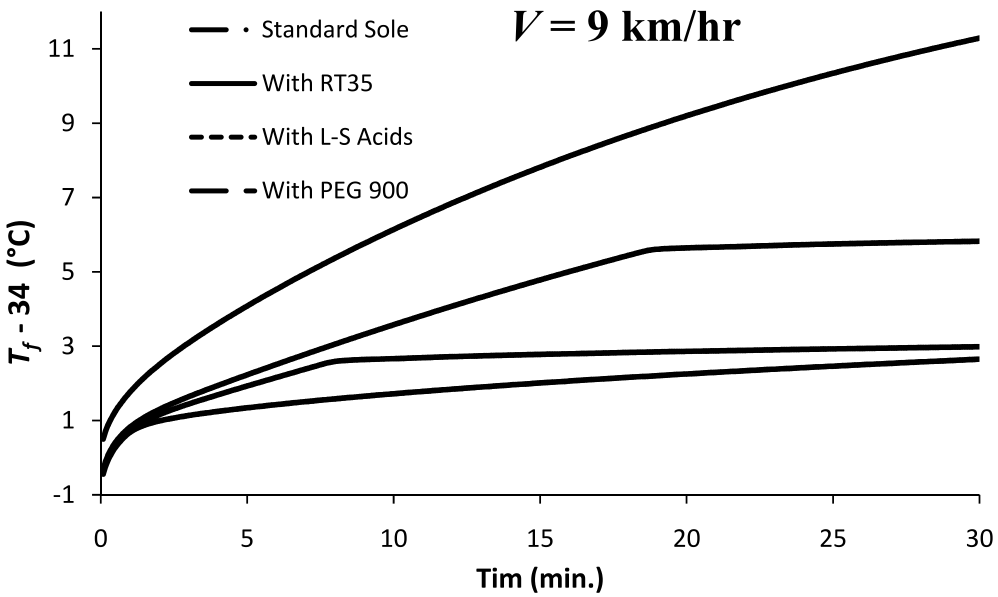

Fig. 4: Comparison of ball temperature rise (standard shoe sole with enhanced shoe soles).

At a running speed as high as 9 km/hr, L-S acid plays a role and prevents a sharp rise in foot temperature. The performance of RT35 is still outstanding. At such a high running speed, the temperature rise is only 2 °C more than this shoe sole at a 3 km/hr speed. Since PEG melts at a single point temperature, at the end of 30 minutes of running, the foot temperature is the same, regardless of the running speed.

PCMs' liquid fractions over time are presented in Fig. 5. Liquid fraction is defined as the mass percent of liquid PCM and shows how much PCM is melted. $\gamma = 0$ means PCM is in the solid state while $\gamma = 1$ means PCM is totally melted. This figure shows that for the worst case, the liquid fraction is less than 14%. It means that there is still enough capacity for heat storage in warmer climates or worse conditions. Moreover, this extra PCM brings flexibility to the mechanical design of the porous layer. In other words, the porosity can be reduced without losing the thermal performance of the enhanced shoe sole.

Comparing the performances of these enhanced shoe soles shows that:

- L-S acid is activated only in high-speed running. Since its melting temperature is high, it is not so effective. At the end of the experiment, a small value of L-S acid melts.
- RT35 has the lowest melting temperature and consequently, it plays the cooling role even at the lowest jogging speed. Since it has a melting temperature range, it slows down the foot sole temperature increase and limits it to less than 4 °C (from -1 °C to 3 °C at 9 km/hr).
- PEG 900 has a single melting temperature. So, at the beginning of running, it does not melt effectively and only its sensible heat is working. So, the temperature relatively rises sharply. But very soon, it stabilizes the temperature of the foot at a constant value. In this respect, the performance of PEG is similar to RT35.

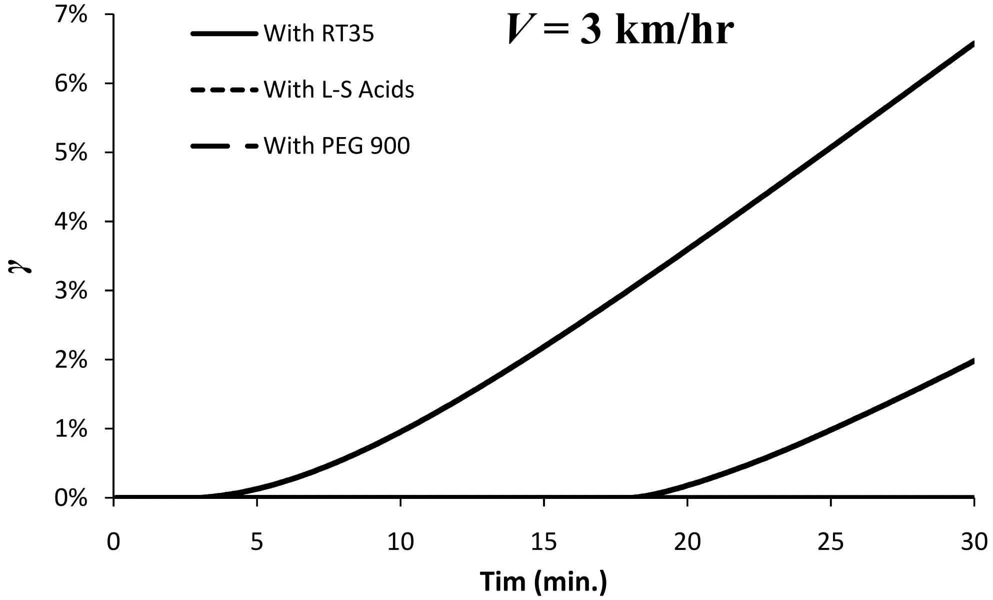

$V = 3$ km/hr
With RT35
With L-S Acids
With PEG 900
7%
6%
5%
4%
3%
2%
1%
0%
γ
0
5
10
15
20
25
30
Tim (min.)

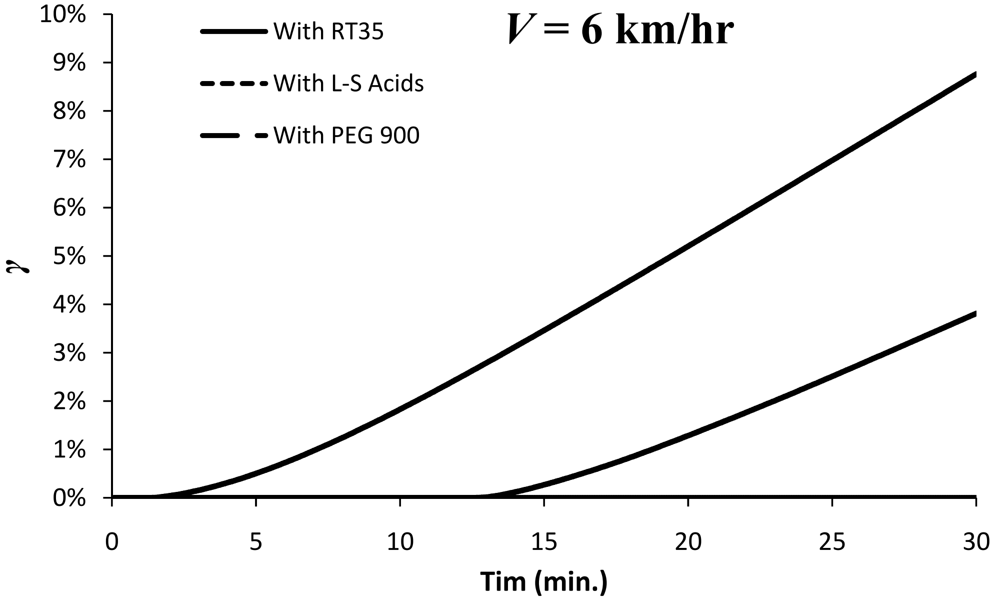

$V = 6$ km/hr
With RT35
With L-S Acids
With PEG 900
10%
9%
8%
7%
6%
5%
4%
3%
2%
1%
0%
γ
0
5
10
15
20
25
30
Tim (min.)

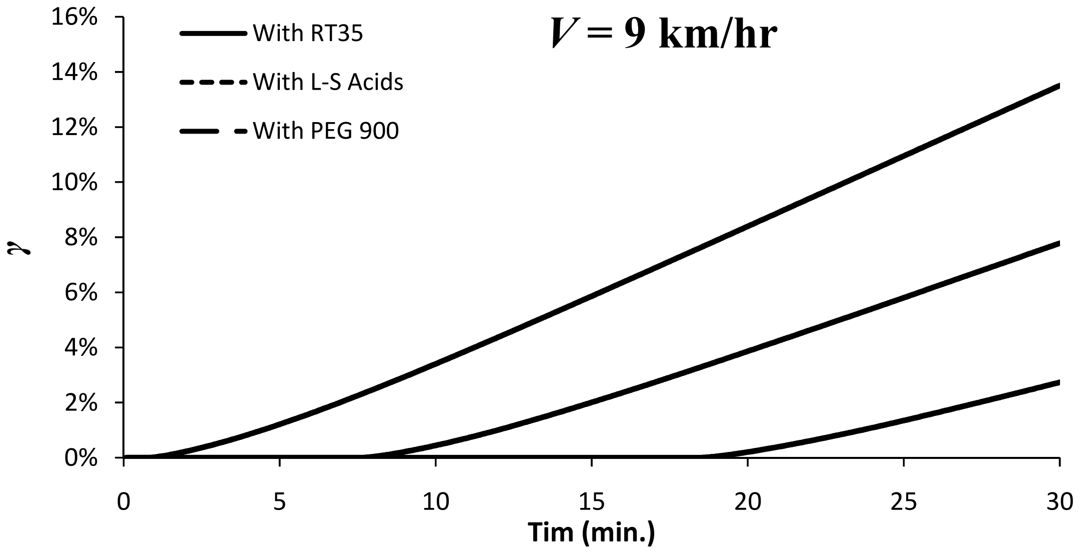

Fig. 5: PCM liquid mass fraction during running time.

4. Conclusions

The high risk of injuries due to load-bearing activities (especially in diabetics) at high foot plantar temperature necessitates the design of a comfortable shoe sole from both thermal and mechanical points of view. It is not always possible to gather suitable thermal and mechanical properties in a single shoe sole structure. For this reason, in this study, a PCM-enhanced shoe sole was proposed. In this sole, a structured-porous layer, filled with PCM is embedded in the sole. Results show a considerable reduction in foot sole temperature increase. In this study, three PCM were selected, i.e. RT35 (paraffin wax), L-S acids (Lauric-Stearic acids), and PEG 900. All of these PCMs have low melting temperatures. The first one has a narrow-range melting temperature while the rest have single-point melting temperatures.

Results show:

- Because the sensible heat capacity of the PCM is higher than the shoe sole, at the beginning of the running, the foot sole temperature is colder by almost 1 °C.

- RT35 and PEG 900 show excellent performance and can keep the foot sole cool during walking and even more intense activities such as jogging and running.
- Due to the relatively high melting temperature of L-S acid, it is activated only at high running speed.
- With an enhanced shoe sole, foot sole temperature increases less than 4 °C even in running with a speed of 9 km/hr.
- After running for 30 minutes at the speed of 9 km/hr (the most exothermic activity in this study), only 14% of RT35 melted. It shows that there is a high capacity for absorbing heat for a longer time.

This study showed that without a noticeable change in shoe sole weight and mechanical properties, the PCM-enhanced shoe sole can be used to regulate foot temperature to prevent the risk of injuries due to hyperthermia especially, for the diabetic feet.

5. Nomenclature

A	Area [m^2]
c_p	Specific heat [J/kgK]
F	Metabolism intensification factor
$\vec{g}$	gravity vector [m/s^2]
H	Enthalpy [J/kg]
h	Average convective heat transfer coefficient [W/m^2 K]
k	Thermal conductivity [W/mK]
L	Latent heat [J/kg]
l	Shoe length [m]
P	Pressure [Pa]
Pr	Prandtl number
q''	Heat flux [W/m^2]
Re	Reynolds number
S	Source term in the momentum equation
T	Temperature [K]
V	Gait speed [m/s]
$\vec{v}$	Velocity vector [m/s]
x, y, z	Cartesian coordinate axis

Greek letters

α	Thermal diffusivity [m^2/s]
β	Thermal expansion coefficient [1/K]
γ	liquid fraction
μ	Viscosity [Pa.s]

ρ	Density [kg/m^3]
τ	Time [s]

Subscripts

a	Air
amb	Ambient
conv	Convection
l	Melting
met	Metabolism
ref	Reference
s	Shoe sole, solidification
∞	Ambient

6. References

[1] H. Rintamäki, S. Rissanen, T. Mäkinen, A. Peitso, Finger temperatures during military field training at 0 to− 29 C, Journal of Thermal Biology 29(7-8) (2004) 857-860.

[2] I. Klarzak, E. Ura-Bińczyk, M. Płocińska, M. Jurczyk-Kowalska, Effect of temperature and humidity on heat effect of commercial chemical warmers based on iron powder, Thermal Science and Engineering Progress 6 (2018) 87-94.

[3] S. James, Encyclopaedia of Occupational Health and Safety 4th edition, Reference Reviews (1999).

[4] N.A. Taylor, C.A. Machado-Moreira, A.M. van den Heuvel, J.N. Caldwell, Hands and feet: physiological insulators, radiators and evaporators, European journal of applied physiology 114(10) (2014) 2037-2060.

[5] S. Mahjoob, K. Vafai, Analytical characterization of heat transport through biological media incorporating hyperthermia treatment, International Journal of Heat and Mass Transfer 52(5-6) (2009) 1608-1618.

[6] A. AlAmiri, K. Khanafer, K. Vafai, Fluid-structure interactions in a tissue during hyperthermia, Numerical Heat Transfer, Part A: Applications 66(1) (2014) 1-16.

[7] S. Chung, K. Vafai, Mechanobiology of low-density lipoprotein transport within an arterial wall—impact of hyperthermia and coupling effects, Journal of biomechanics 47(1) (2014) 137-147.

[8] H. Kinoshita, B.T. Bates, The effect of environmental temperature on the properties of running shoes, Journal of applied biomechanics 12(2) (1996) 258-268.

[9] A. Ersen, L.S. Adams, R.T. Myers, G.B. Hirschman, L.A. Lavery, M. Yavuz, Temperature Regulating Shoes for Prevention of Diabetic Foot Ulcers, Am Diabetes Assoc, 2018.

[10] V.J. Houghton, V.M. Bower, D.C. Chant, Is an increase in skin temperature predictive of neuropathic foot ulceration in people with diabetes? A systematic review and meta-analysis, Journal of foot and ankle research 6(1) (2013) 31.

[11] M. Yavuz, A. Ersen, A. Monga, L.A. Lavery, A.G. Garrett, Y. Salem, G.B. Hirschman, R. Myers, Temperature-and Pressure-Regulating Insoles for Prevention of Diabetic Foot Ulcers, The Journal of Foot and Ankle Surgery 59(4) (2020) 685-688.

[12] E. Arce, R. Devesa-Rey, A. Suárez-García, D. González-Peña, M. García-Fuente, Effect of Phase-Change Materials on Laboratory-Made Insoles: Analysis of Environmental Conditions, Materials 15(19) (2022) 6967.

[13] K.-l. Yick, A. Yu, P.-l. Li, Insights into footwear preferences and insole design to improve thermal environment of footwear, International Journal of Fashion Design, Technology and Education 12(3) (2019) 325-334.

[14] Y. Shimazaki, M. Murata, Effect of gait on formation of thermal environment inside footwear, Applied ergonomics 49 (2015) 55-62.

[15] Y. Shimazaki, T. Matsutani, Y. Satsumoto, Evaluation of thermal formation and air ventilation inside footwear during gait: The role of gait and fitting, Applied ergonomics 55 (2016) 234-240.

[16] Y. Shimazaki, S. Nozu, T. Inoue, Shock-absorption properties of functionally graded EVA laminates for footwear design, Polymer Testing 54 (2016) 98-103.

[17] Y. Shimazaki, K. Aisaka, Novel Thermal Analysis Model of the Foot-Shoe Sole Interface during Gait Motion, Multidisciplinary Digital Publishing Institute Proceedings, 2018, p. 278.

[18] H. Nemati, M. Moghimi, R. Naemi, A mathematical model to investigate heat transfer in footwear during walking and jogging, Journal of Thermal Biology 97 (2021) 102778.

[19] H. Nemati, R. Naemi, An Analytical Model to Predict Foot Sole Temperature: Implications to Insole Design for Physical Activity in Sport and Exercise, Applied Sciences 12(13) (2022) 6806.

[20] H. Nemati, M. Habibi, Analytical and numerical analysis of phase change material solidification in partially filled capsules considering breathing vent, Journal of Energy Storage 40 (2021) 102725.

[21] M.S. Mahdi, H.B. Mahood, A.A. Alammar, A.A. Khadom, Numerical investigation of PCM melting using different tube configurations in a shell and tube latent heat thermal storage unit, Thermal Science and Engineering Progress 25 (2021) 101030.

[22] E. Cihan, H.K. Berent, H. Demir, H.F. Öztop, Entropy analysis and thermal energy storage performance of PCM in Honeycomb Structure: Effects of materials and dimensions, Thermal Science and Engineering Progress (2023) 101668.

[23] H. Nemati, V. Souriaee, M. Habibi, K. Vafai, Design and Taguchi-based optimization of the latent heat thermal storage in the form of structured porous-coated pipe, Energy 263 (2023) 125947.

[24] H.B. Mahood, M.S. Mahdi, A.A. Monjezi, A.A. Khadom, A.N. Campbell, Numerical investigation on the effect of fin design on the melting of phase change material in a horizontal shell and tube thermal energy storage, Journal of Energy Storage 29 (2020) 101331.

[25] A. Kumar, Rajeev, A Stefan problem with moving phase change material, variable thermal conductivity and periodic boundary condition, Applied Mathematics and Computation 386 (2020) 125490.

[26] L. Jain, A. Kumar, Rajeev, A numerical study of a moving boundary problem with mixed boundary condition and variable thermal coefficients, Computational Thermal Sciences: An International Journal 12(3) (2020).

[27] A.K. Singh, A. Kumar, Rajeev, Exact and approximate solutions of a phase change problem with moving phase change material and variable thermal coefficients, Journal of King Saud University-Science 31(4) (2019) 1318-1325.

[28] S. Das, Rajeev, An approximate analytical solution of one-dimensional phase change problems in a finite domain, Applied mathematics and computation 217(13) (2011) 6040-6046.

[29] A. Brent, V.R. Voller, K. Reid, Enthalpy-porosity technique for modeling convection-diffusion phase change: application to the melting of a pure metal, Numerical Heat Transfer, Part A Applications 13(3) (1988) 297-318.

[30] H.K. Versteeg, W. Malalasekera, An introduction to computational fluid dynamics: the finite volume method, Pearson education2007.

[31] G. Chen, G. Sun, D. Jiang, Y. Su, Experimental and numerical investigation of the latent heat thermal storage unit with PCM packing at the inner side of a tube, International Journal of Heat and Mass Transfer 152 (2020) 119480.

[32] T.L. Bergman, F.P. Incropera, A.S. Lavine, D.P. DeWitt, Introduction to heat transfer, John Wiley & Sons2011.

[33] D. Rozanna, T. Chuah, A. Salmiah, T.S. Choong, M. Sa'Ari, Fatty acids as phase change materials (PCMs) for thermal energy storage: a review, International journal of green energy 1(4) (2005) 495-513.

[34] N.R. Jankowski, F.P. McCluskey, A review of phase change materials for vehicle component thermal buffering, Applied energy 113 (2014) 1525-1561.

[35] GmbH, Rubitherm Technologies GmbH: Datasheet RT35, from: https://www.rubitherm.eu/media/products/datasheets/Techdata_-RT35_EN_02092022.PDF.

[36] K. Tuncbilek, A. Sari, S. Tarhan, G. Ergüneş, K. Kaygusuz, Lauric and palmitic acids eutectic mixture as latent heat storage material for low temperature heating applications, Energy 30(5) (2005) 677-692.

[37] Y. Wang, A. Amiri, K. Vafai, An experimental investigation of the melting process in a rectangular enclosure, International Journal of Heat and Mass Transfer 42(19) (1999) 3659-3672.

[38] A. Sari, K. Kaygusuz, Thermal performance of a eutectic mixture of lauric and stearic acids as PCM encapsulated in the annulus of two concentric pipes, Solar Energy 72(6) (2002) 493-504.